Dynactin targets Pavarotti-KLP to the central spindle during anaphase and facilitates cytokinesis in *Drosophila* S2 cells

Jean-Guy Delcros, Claude Prigent and Régis Giet*

CNRS UMR 6061 'Génétique et Développement', Groupe Cycle Cellulaire, Faculté de Médecine, IFR 140 Génomique Fonctionnelle et Santé, Université de Rennes I, 2 avenue du Pr. Léon Bernard, CS 34317, F-35043 Rennes CEDEX, France

*Author for correspondence (e-mail: regis.giet@univ-rennes1.fr)

Accepted 8 August 2006
Journal of Cell Science 119, 4431-4441 Published by The Company of Biologists 2006
doi:10.1242/jcs.03204

Summary

The dynactin complex cooperates with the dynein complex in various systems for mitotic completion. Here we analysed the mitotic phenotype of *Drosophila* S2 cells following the knockdown of the dynactin subunit p150^{Glued}. We found that p150^{Glued}-depleted cells were delayed in metaphase and that the centrosomes were poorly connected to mitotic spindle poles. In addition, anaphase occurred with asynchronous chromosome segregation. Although cyclin B was degraded in these anaphase cells, Aurora B, MEI-S322 and BubR1 were not released from the non-segregating chromosomes. We also found that the density and organisation of the central spindle were compromised, with Aurora B and polo kinases absent from the diminished number of microtubules. Pavarotti-KLP, a component of the centralspindlin complex required for the formation of stable microtubule bundles, was not immediately targeted to the plus ends of the microtubules following anaphase onset as happened in controls. Instead, it accumulated transiently at the cell cortex during early anaphase and its targeting to the central spindle was delayed. These data suggest that the dynactin complex contributes to cytokinesis by promoting stable targeting of the centralspindlin complex to microtubule plus ends at anaphase onset. The contribution of the dynein-dynactin complex to synchronous chromosome segregation and cytokinesis is discussed.

Supplementary material available online at
http://jcs.biologists.org/cgi/content/full/119/21/4431/DC1

Key words: Dynactin, Mitosis, Cytokinesis

Introduction

Dynein is a microtubule motor that moves toward the minus end of microtubules as part of a large macromolecular complex (Collins and Vallee, 1989; Vallee et al., 1989). This complex has many functions. It is involved in the transport of molecules and organelles along microtubules during interphase and nuclear positioning (Karki and Holzbaur, 1999). Cytoplasmic dynein, which is present at the cell cortex, pulls on centrosome-connected microtubules and is responsible for the positioning of the centrosomes in the centre of the cell (Koonce et al., 1999; Vallee and Stehman, 2005). The same principle is used in yeast cells to pull newly duplicated nuclei into the bud and in mitotic vertebrate cultured cells, as well as in *Drosophila* and *Caenorhabditis elegans* somatic tissues, to pull the centrosomes apart during prophase (Busson et al., 1998; Carminati and Stearns, 1997; Koonce et al., 1999; Vallee and Stehman, 2005; Gonczy et al., 1999; Robinson et al., 1999; Schmidt et al., 2005).

The dynein complex can be isolated biochemically with dynactin, a 20S multi-protein complex containing at least ten proteins (Karki and Holzbaur, 1999). In vitro, the dynactin complex stimulates the dynein motor activity (Gill et al., 1991). It has been suggested that one major function of dynactin is to target dynein where it is required in the cell (Vallee et al., 1995).

The *Glued* gene encodes a 150 kDa protein that belongs to the dynactin complex. In fission yeasts and in humans, p150^{Glued} regulates microtubule dynamics (Niccoli et al., 2004). In human cells, this regulation depends on association with EB1 and is essential to maintain the radial arrays of microtubules in interphase cells (Askham et al., 2002; Strickland et al., 2005). A recent study further proposed that the interaction between EB1 and p150^{Glued} promotes the elongation of astral microtubules to facilitate furrow ingression during cytokinesis (Strickland et al., 2005).

When cells enter mitosis and prophase, dynein facilitates nuclear envelope breakdown for spindle formation: it pulls nuclear membranes and associated proteins poleward along astral microtubules leading to nuclear membrane detachment (Salina et al., 2002). During prometaphase, it has been clearly demonstrated in *Drosophila* and human cultured cells, that the dynein-dynactin complex (DDC) is continuously recruited to the kinetochores until they become properly attached to the mitotic spindle. Kinetochore dynein then moves towards the spindle poles thereby removing checkpoint proteins and allowing the inactivation of the spindle checkpoint and the anaphase onset (Karess, 2005). In addition, mutations that affect dynein loading at the kinetochore, lead to asynchronous chromosome segregation and attenuated chromosome motion toward the poles (Savoian et al., 2000; Sharp et al., 2000). In

Drosophila, interfering with dynein-dynactin functions using antibodies or RNAi also induces the detachment of the centrosomes from the spindle poles (Goshima and Vale, 2003; Goshima and Vale, 2005; Morales-Mulia and Scholey, 2005).

Here, using RNAi for the *Glued* gene in *Drosophila* S2 cells, we confirm that *Glued* is required for centrosome connection to spindle poles, the metaphase-to-anaphase transition, and synchronous chromosome-to-pole movement during anaphase. In addition, we report that the dynactin complex also facilitates cytokinesis by targeting Pavarotti-KLP, a component of the centralspindlin complex, to the plus ends of central spindle microtubules.

Results

p150^{Glued} localises to centrosomes, mitotic spindle microtubules and kinetochores

Two antisera raised against the first 148 amino acids of the p150^{Glued} polypeptide were produced in rabbits (Rb1477 and Rb1478). These two antisera recognised a common protein at 150 kDa, the expected size of the p150^{Glued} protein in *Drosophila* S2 cell extracts as well as one or more other bands (Fig. 1A). After affinity purification, only a single 150 kDa protein could be detected (Fig. 1A, lane AP). The p150^{Glued} protein signal disappeared following *Glued* RNAi of S2 cells whereas loading control proteins, cyclin B, aurora A, CP190 and dynein intermediate chain (DIC) remained stable (Fig. 1B, compare lanes – and lanes +), further demonstrating the specificity of our antibodies.

The anti-p150^{Glued} affinity-purified antibody was used to stain cultured *Drosophila* S2 cells and embryos (Fig. 2). During prophase, the antibody decorated the two asters of microtubules (Fig. 2A, panel p). During metaphase, labelling was observed on centrosomes/asters as well as on spindle microtubule fibres (panel m). From anaphase until cytokinesis, p150^{Glued} was detected on the astral and central spindle microtubules (Fig. 2A, panels a,c). In interphase cells, we found a punctuated p150^{Glued} labelling in the cytoplasm and along microtubule fibres (Fig. 2B) as observed previously in human cells (Vaughan et al., 2002). We further observed paired-dot-like staining on some metaphase chromosomes. This staining became more evident when microtubules were depolymerised with colchicine and furthermore, co-localised with polo kinase, a known kinetochore component (Fig. 2D). Thus, like the dynein motor protein, p150^{Glued} associates with kinetochores. To further examine the distribution of p150^{Glued} during mitosis, we stained syncitial embryos (Fig. 2C). In agreement with our findings in cultured cells, p150^{Glued} first associated with prophase asters and the subsequent metaphase and anaphase spindles.

We next attempted to examine the dynamics of p150^{Glued} in living cells using a GFP-tagged transgene. However, despite the use of the ubiquitin promoter to drive expression (see Materials and Methods) the fluorescence intensity of GFP-p150^{Glued} was too weak to be detected in live material. Therefore a GFP antibody was used to stain fixed expressing cells. GFP labelling was detected on the centrosomal region and the spindle microtubules during mitosis, as well as at the midbody region during cytokinesis (supplementary material Fig. S1). Thus, a combination of GFP-tagging and immunofluorescence studies demonstrated that the p150^{Glued} protein shares a common localisation in both S2 cells and syncitial embryos; it associates with centrosomes, microtubules and kinetochores. In addition, the p150^{Glued} protein was also detected on the central spindle microtubules and the midbody during late telophase and cytokinesis.

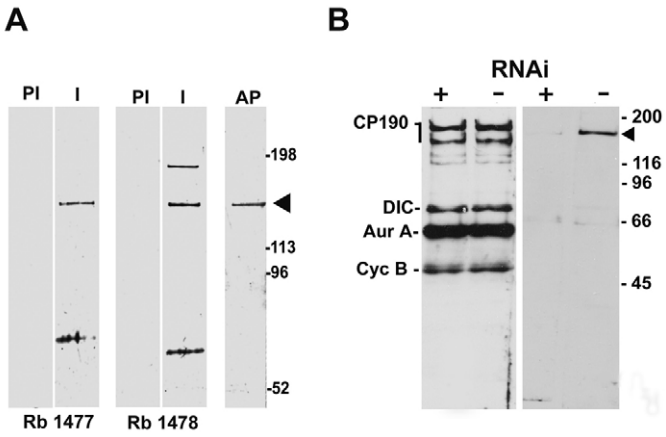

Fig. 1. p150^{Glued} antibodies. (A) S2 cell extracts were probed with pre-immune (PI), immune (I) sera Rb1477(left), Rb1478 (middle) or affinity-purified antibodies (right, AP). The position of the p150^{Glued} protein is indicated with the arrowhead. (B) Extracts from S2 cells treated (+) or not (–) with *Glued* dsRNA were analysed with CP190, aurora A, cyclin B and dynein intermediate chain (DIC) antibodies (left) as loading controls, as well as with the affinity-purified anti-p150^{Glued} antibodies (right).

Mitotic defects following *Glued* RNAi

To monitor the contribution of *Glued* during mitosis in *Drosophila* S2 cells, we performed RNAi against the *Glued* mRNA transcript, and mitotic cells were fixed and analysed by immunofluorescence microscopy (Table 1 and Fig. 3). Three to four days post-transfection with *Glued* dsRNA, p150^{Glued} protein levels were greatly reduced as evidenced by western blot analyses (Fig. 1B). Mitotic indices were four times higher in p150^{Glued}-depleted cells compared with control cells. Of these, the proportion of cells at metaphase (60.5%) was significantly greater than in controls (29.2%). In addition, the number of abnormal mitotic anaphase cells was five times greater in p150^{Glued} knock down cells (see below).

Table 1. Quantification of the mitotic defects in control or *Glued* RNAi S2 cells

	Mitotic index	Prophase*	Metaphase*	Anaphase + telophase*	Cytokinesis*	Abnormal spindles*,‡	Abnormal anaphases*
Control RNAi	3.0±1.5	8.1±1.9	29.2±5.3	9.4±1.9	41.1±3.8	11.9±2.9	0.3±0.5
Glued RNAi	12.0±3.9	4.5±1.3	60.5±4.8†	2.0±1.7	23.7±1.2	4.5±1.9	4.9±1.2

*Values are the mean percentage of the total number of mitotic cells in each phase (± s.d.). †50% of these spindles show centrosome disconnection from spindle poles. ‡These cells include monopolar, monoastral bipolar and multipolar spindles.

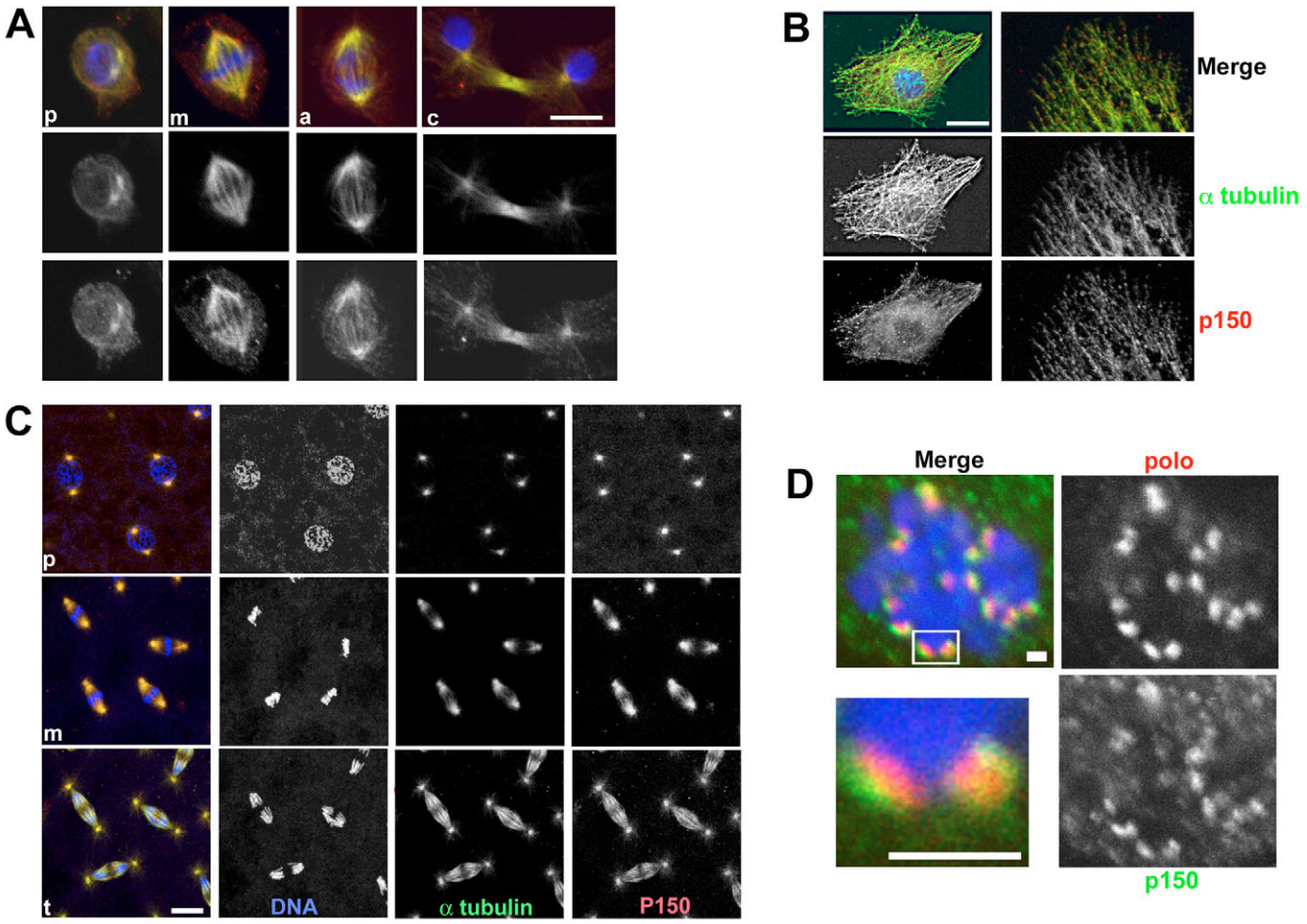

Fig. 2. p150^{Glued} localises to centrosomes, spindle and interphase microtubules. S2 cells (A and B) or early *Drosophila* syncitial embryos (C) were fixed and stained with the affinity-purified anti-p150^{Glued} antibodies (red and lower panels in monochrome), the anti-α-tubulin antibody (green and middle panels in monochrome) and DAPI (DNA staining in blue). (A) Mitotic cells. (B) Interphase cells: the right column shows a 10× magnified view of the border of a flat S2 cell. Note the punctuate staining along microtubule fibres. a, anaphase; c, cytokinesis; m, metaphase; p, prophase; t, telophase. (D) A mitotic cell treated with colchicine to depolymerise the mitotic spindle was stained for polo kinase (red and upper right panel in monochrome) and p150^{Glued} (green and lower panel on the right in monochrome). The lower left panel shows a 10× magnification view of the kinetochore region boxed in the panel above. Bars, 10 μm (A-C); 1 μm (D).

In 50% of the cases, RNAi-treated metaphase cells had normal spindle morphology and could not be differentiated from control cells (Fig. 3B, panel 1). However, the other half of the metaphase cells displayed a weak connection or clear separation between the centrosomes and the spindle poles (Fig. 3B, panel 2), a phenotype also observed after dynein or dynactin interference (Goshima et al., 2005; Morales-Mulia and Scholey, 2005; Siller et al., 2005). The major defect observed following p150^{Glued} RNAi occurred during anaphase, where 4.9% of cells were abnormal compared with 0.3% of control cells. These defects were manifest as gross morphological spindle defects and chromosome segregation errors. In most cases, the spindle appeared abnormally elongated with some chromosomes located at the spindle poles whereas others were still at the spindle equator, suggesting asynchronous chromosome separation. (Fig. 3B, lower panels 3 and 4). During early anaphase, as judged by the separation of the two chromatid masses, the central spindle microtubule density was less robust and lacked the symmetry observed in controls (Fig. 3B, middle panels 3 and 4). In telophase, a disorganised region of equatorial microtubules was able to form, but this region was lacking the well-organised stable anti-parallel microtubule bundles seen in control telophase cells (Fig. 3, compare B panel 5 with A panel t). The FACS analyses showed the absence of polyploid cells in the *Glued* dsRNA-treated cells, but an increase of apoptotic and/or aneuploid cells was detected (Fig. 3C, arrow) suggesting that despite the formation of normal anaphase cells, cytokinesis occurred normally. In all depleted anaphase cells, the chromosomes showed a dot-like morphology suggesting an overcondensation of chromosomes and hence mitotic arrest, as expected from the elevated mitotic index (Table 1).

To confirm that these elongated spindles represented anaphase cells and not aberrant prometaphase cells with congression defects, we monitored the degradation of cyclin B in control and *Glued* dsRNA-treated cells at the metaphase-anaphase transition. Cyclin B levels were high in wild-type and *Glued* dsRNA-treated cells during metaphase and the protein accumulated strongly at centrosomes, spindles and, to a lesser extent, at some kinetochores (Fig. 4, left panels A and B).

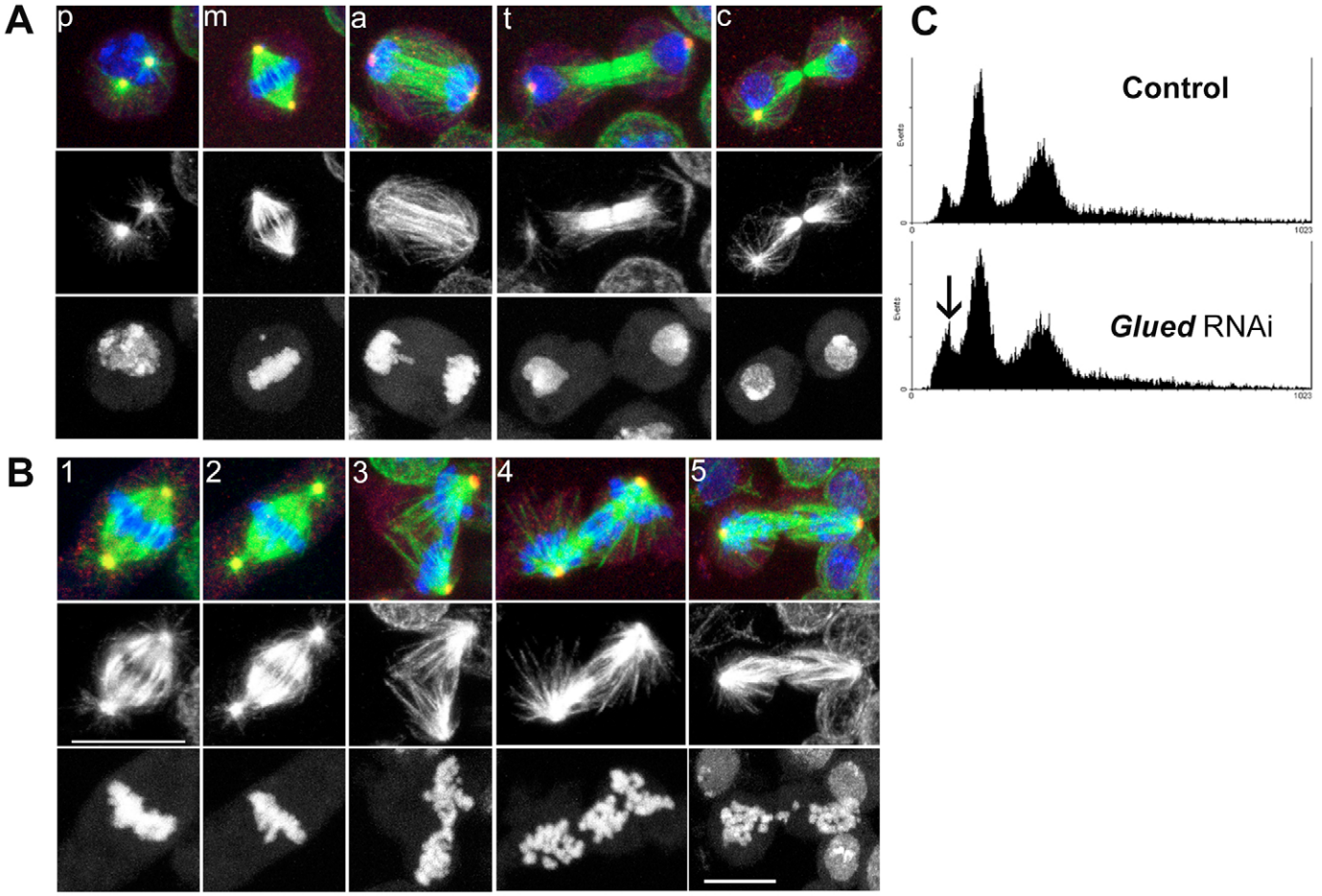

Fig. 3. *Glued* RNAi leads to anaphase defects. Control (A) or *Glued* dsRNA-treated (B) mitotic S2 cells were fixed and stained for γ-tubulin (red), α-tubulin (green and middle panels in monochrome) and DNA (blue and lower panels in monochrome). a, anaphase; c, cytokinesis; m, metaphase; p, prophase; t, telophase. In $p150^{Glued}$-depleted cells, cells are delayed in metaphase (see also Table 1). 50% of these cells show weak centrosome connection to spindle poles (panel 2) whereas others show a normal shape (panel 1). Note the segregation defect and the absence of microtubule bundling during anaphase (panels 3 and 4). During telophase, a central spindle forms but with strongly disorganised microtubules and a lack of well-defined microtubule bundles (panel 5). (C) FACS analysis of *Glued* dsRNA-treated cells does not show any accumulation of polyploid cells but evidences an increase of apoptotic or aneuploid cells (arrow) compared with control cells. Bar, 10 μm.

During anaphase, cyclin B levels were strongly reduced in control cells but some signal was still detected at centrosomes as previously described (Mathe et al., 2004). We consistently found that cyclin B was degraded in *Glued*-depleted cells with elongated spindles and aberrantly positioned chromosomes (Fig. 4A, right panels), indicating that these cells had progressed into anaphase. In addition, we examined the distribution of the MEI-S322 antigen (the *Drosophila* homologue of mammalian shugosin) (Kerrebrock et al., 1995). This protein was released from the centromeres in control anaphase cells and was also lacking at polar-proximal chromosomes in *Glued* dsRNA-treated cells. However, the signal remained quite strong on those chromosomes lagging at the equator (Fig. 4C). Finally we investigated the status of the spindle assembly checkpoint in knockdown cells by staining for the BubR1 antigen. As expected in control cells, BubR1 protein levels were elevated at the kinetochores in early prometaphase cells and much lower in metaphase. The remaining BubR1 protein disappeared following anaphase entry (Karess, 2005). In those RNAi-treated cells exhibiting normal metaphase spindles, all kinetochores appeared to be labelled similarly to control cells. During anaphase, the kinetochores of polar-positioned chromosomes on elongated spindles showed no staining whereas those kinetochores at chromosomes at the centre of the spindle exhibited fluorescence (Fig. 4B). Taken together, these results reveal that the knockdown of $p150^{Glued}$ leads to elongated spindles upon which some chromosomes are able to segregate to the poles during anaphase while others lag at the spindle equator. These lagging chromosomes retain the MEI-S322 centromeric protein as well as the checkpoint component BubR1. Along with these chromosome segregation defects, the central spindle, which normally forms during late anaphase or telophase is greatly diminished, suggesting that $p150^{Glued}$ is needed for central spindle formation or stabilisation.

Aurora B and polo kinases are not recruited to the microtubules in *Glued*-depleted anaphase cells

The failure to form or maintain the central spindle in $p150^{Glued}$-depleted cells prompted us to investigate the distribution of two

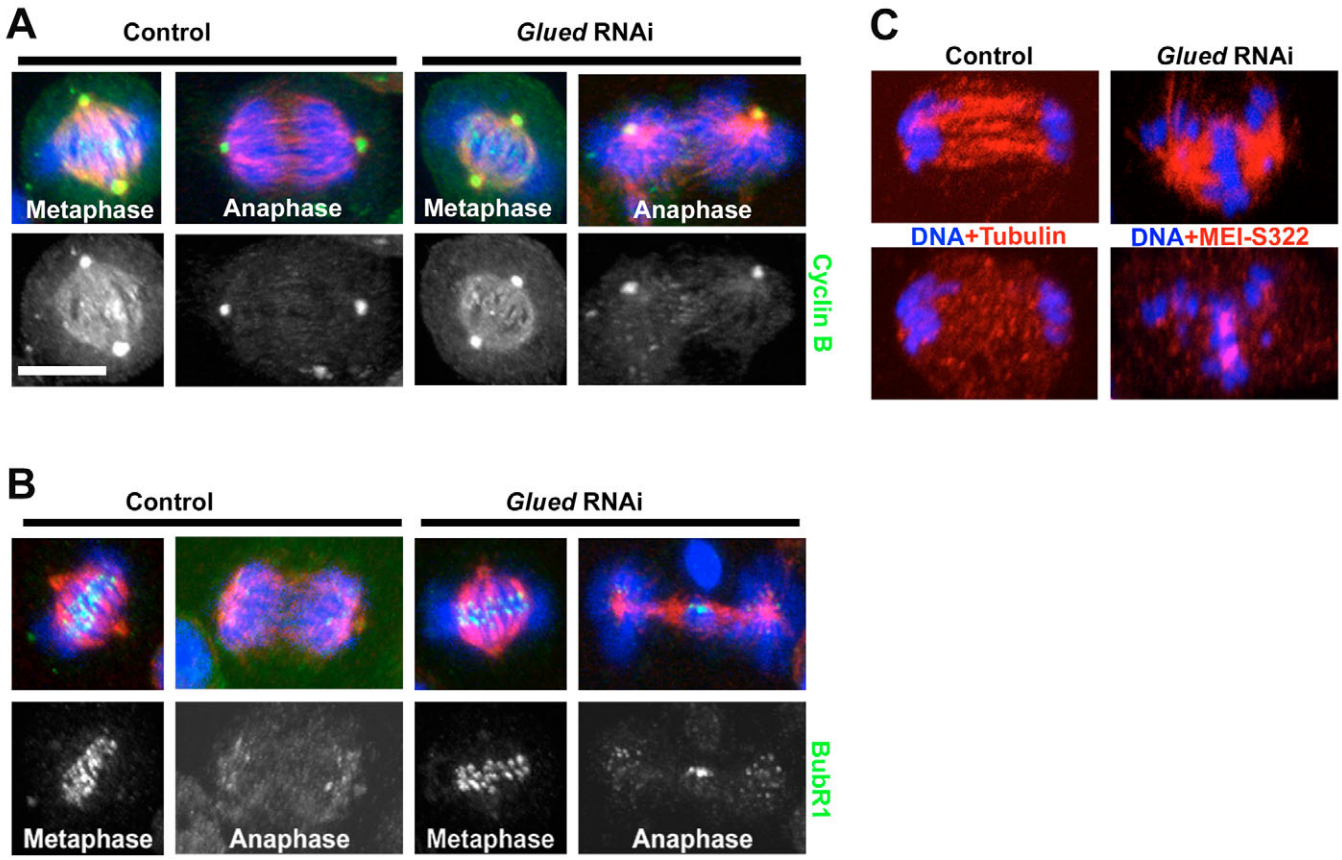

Fig. 4. Cyclin B, BubR1 and MEI-S322 behaviour in *Glued*-depleted anaphases. Control or *Glued* dsRNA-treated S2 cells were cold fixed in methanol (A and B) and stained for Cyclin B (A, green and lower panels in monochrome) and BubR1 (B, green and lower panels in monochrome), tubulin (red) and DNA (blue). Metaphase and anaphase cells are shown. (A) Cyclin B levels are elevated in metaphase and decrease during early anaphase after chromosome segregation. (B) A pool of BubR1 protein remains at the kinetochores of *Glued* or control dsRNA-treated cells during metaphase and is released from the kinetochore at anaphase onset in control cells. Note that BubR1 signal remains elevated at the kinetochore of chromatids that have not segregated in *Glued*-depleted anaphases. (C) MEI-S322 protein releases from the centromeres of $p150^{Glued}$ knockdown anaphase cells. Control (left) or *Glued* dsRNA-treated (right) cells were stained for MEI-S322 protein (red in bottom panels), α-tubulin (red in top panels) and DNA (blue). Note that the MEI-S322 antigen is released in early anaphase cells but persists at the centromeres of unsegregated chromatids during asynchronous chromosome segregation. Bar, 10 μm.

central-spindle-dependent protein kinases. The first of these, Aurora B, is a chromosome passenger protein that localises to the centromeric region of the chromosomes during prophase until metaphase (Fig. 5A, panel 1). This protein then redistributes to the central spindle midzone during anaphase A (Fig. 5A, panel 2), where it remains during anaphase B (panel 3) and telophase (panel 4) and is needed to stabilise central spindle microtubules for successful cytokinesis (Giet and Glover, 2001).

In *Glued* RNAi-treated cells, Aurora B still localised to the centromeric region of mitotic chromosomes during metaphase (Fig. 5B, panel 1). In post-anaphase cells Aurora B was not detected on the centromeres of those chromosomes that had successfully migrated to the poles. However, it was retained at the centromeres of those chromosomes that failed to segregate (Fig. 5B, panels 2 and 3). Thus, Aurora B behaved exactly like the MEI-S322 and BubR1 proteins during asynchronous anaphases. The levels of Aurora B in these centromeres were similar but sometimes higher than the levels seen in the centromeres of control or $p150^{Glued}$-depleted metaphase cells (see supplementary material Fig. S2 for comparison). We next examined the distribution of Aurora B in those cells where the chromosomes had successfully segregated but no discrete central spindle could be detected. Importantly, we failed to detect any equatorially localised Aurora B in anaphase cells even when the fluorescence signal was over-exposed (Fig. 5B, panels 4), but could sometimes find this kinase on the few central spindle microtubule bundles that formed in later-stage cells. This suggests that Aurora B redistribution to the equator for central spindle formation is less efficient but not entirely inhibited following knockdown of $p150^{Glued}$.

Although the failure of Aurora B to concentrate at the equator in a timely fashion was sufficient to explain the diminished central spindles observed following *Glued* RNAi, we checked the localisation of the polo kinase, another kinase that is crucial for central spindle formation and successful cytokinesis. In anaphase cells, polo localised to the kinetochores of the segregated chomatids (Fig. 6A,B) and at the overlapping plus ends of central spindle microtubules at the midzone. In *Glued* dsRNA-treated cells, polo was also found on segregated kinetochores, but was not detected at the plus ends of predicted central spindle microtubules (Fig. 6C,D). We

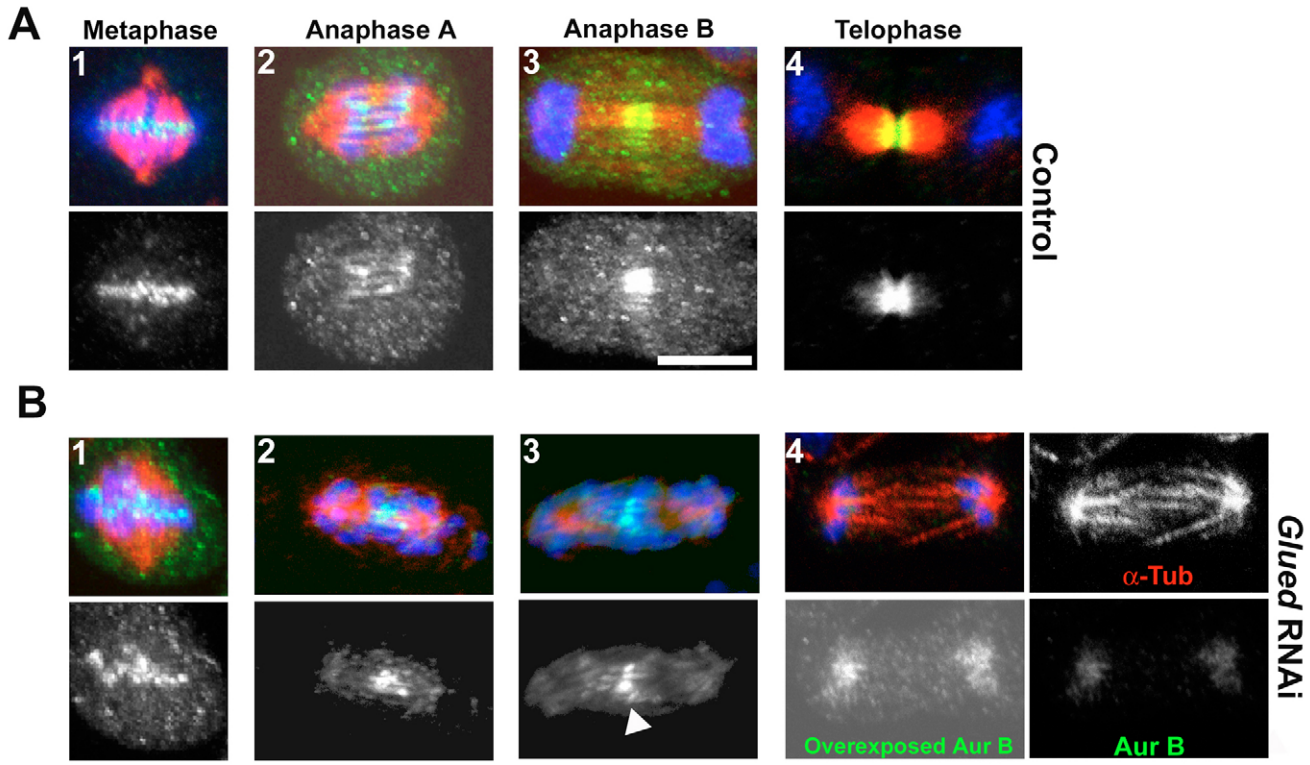

Fig. 5. Aurora B behaviour in p150^{Glued}-depleted anaphases. Control (A) or *Glued* dsRNA-treated (B) S2 cells (B) were fixed and stained for aurora B (green and lower panels in monochrome), tubulin (red and monochrome in top right panel 4) and DNA (blue). In control or p150^{Glued}-depleted metaphase cells (panel 1), aurora B is recruited to the centromeres. During anaphase A (A, panel 2), note the disappearance of aurora B from the centromeres and its progressive relocalisation to the central spindle during anaphase B (panel 3) and telophase (panel 4). In p150^{Glued}-depleted anaphase cells (panels 2 and 3), aurora B is detected at the centromeres (white arrowhead) that have not segregated (see also supplementary material Fig. S2) and there is no recruitment to the microtubules. Panel 4 shows a p150^{Glued}-depleted anaphase cell in which aurora B signal was overexposed (lower left panel) to show that aurora B signal is not detected on the few microtubules seen between the two chromatin masses. Bar, 10 μm.

confirmed that the knockdown cells had progressed beyond metaphase by staining for Cyclin B (green), which further allowed us to discriminate the boundaries of the cell (shown in white). As can be seen in the figure, along with the spindle defects described above, knockdown cells have abnormal cortices that are distorted and buckled. This may reflect unregulated cortical contractions during this late mitotic stage.

Glued RNAi cells lack stable microtubule bundles and Pavarotti-KLP

To further define the central spindle defects associated with p150^{Glued} depletion, we examined the distribution of Pavarotti-KLP. This motor protein is part of the evolutionarily conserved centralspindlin complex that has been implicated as a major player in both central spindle formation and cleavage furrow

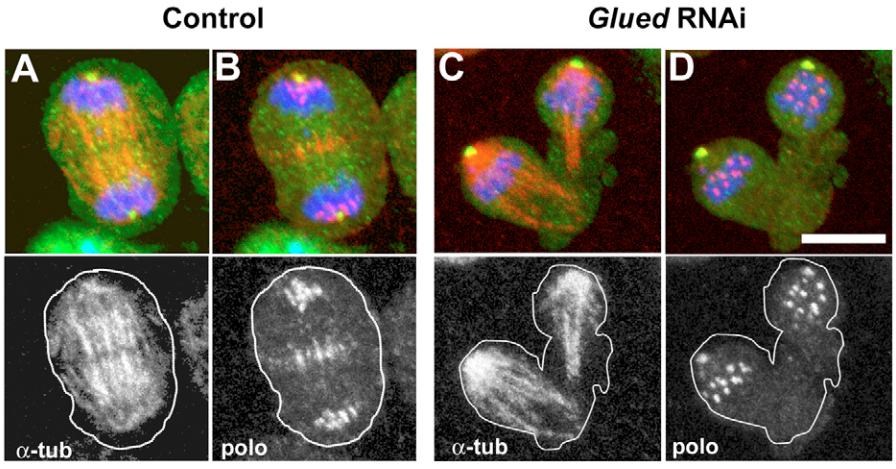

Fig. 6. Polo protein kinase behaviour in p150^{Glued}-depleted anaphases. Wild-type (A,B) and *Glued* RNAi (C,D) cells during anaphase were fixed and stained for cyclin B (green), polo (red, in panels B and D, and lower panels in monochrome), and α-tubulin (red in panels A and C, and lower panels in monochrome. In control anaphase (B), polo localises to the kinetochores and on central spindle microtubules. In *Glued* dsRNA-treated cells (D), polo is detected on the kinetochores but not on the microtubules present between the two chromatid masses. Note also the abnormal cortex contraction in this cell (white line). Bar, 10 μm.

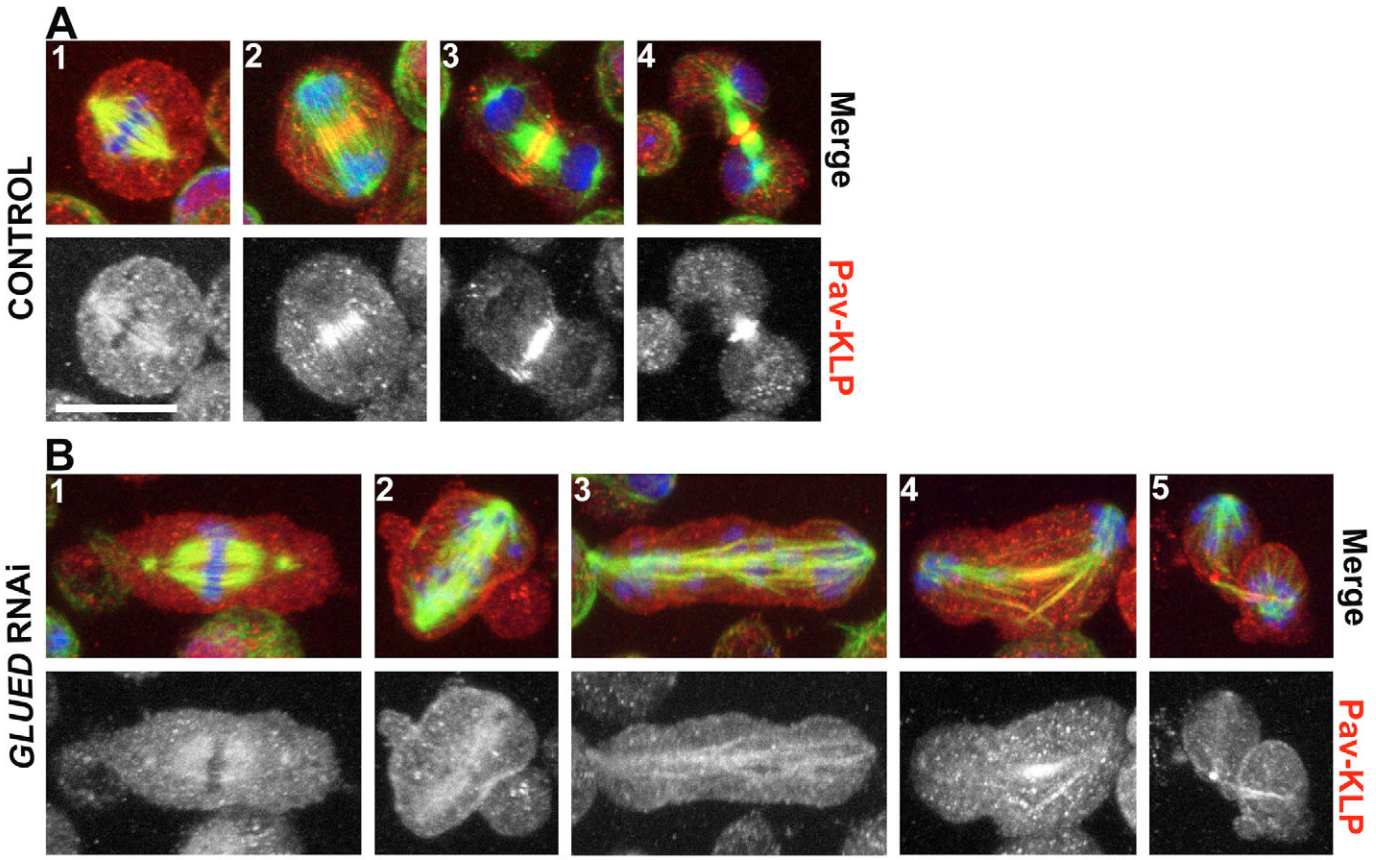

Fig. 7. Pavarotti-KLP targeting to the plus ends of microtubules and central spindle formation is delayed in *Glued* dsRNA-treated cells. Control or *Glued* dsRNA-treated mitotic cells were stained for Pavarotti-KLP (red and lower panels in monochrome), DNA (blue) and microtubules (green). (A) Pavarotti-KLP faintly localises to the mitotic spindle during metaphase (panel 1) and strongly accumulates at the plus ends of microtubules during anaphase (panel 2), telophase (panel 3) and the midbody during cytokinesis (panel 4). (B) Pavarotti-KLP localises to the mitotic spindle in a $p150^{Glued}$ knockdown metaphase cell (panel 1) but is not relocalised to microtubule plus ends during anaphase and transiently accumulates at the cell periphery where cortex contractions are detected (panel 2). As the cell progresses through anaphase-B-telophase, Pavarotti-KLP starts to accumulate on the microtubules present between the two chromatid masses (panel 3) allowing a reduced central spindle to form (panel 4) and cytokinesis to occur (panel 5). Bar, 10 μm.

initiation in different organisms. This protein localises to microtubule plus ends after anaphase onset and is required for microtubule bundling and central spindle formation (Adams et al., 1998). In control cells, Pavarotti-KLP was detected on spindle microtubules during metaphase (Fig. 7A, panel 1). At anaphase onset, the protein concentrated at the plus ends of central spindle microtubules where it persisted until cytokinesis was completed (Fig. 7A, panels 2-4). Likewise, in *Glued* RNAi-treated cells Pavarotti-KLP was detected on the metaphase spindle (Fig. 7B, panel 1). Following the metaphase-to-anaphase transition, we found that Pavarotti-KLP did not concentrate into a tight aggregate at the plus ends of microtubules regardless of the presence or absence of lagging chromosomes. Interestingly, Pavarotti-KLP often appeared less intense at polar regions, although the significance of this remains unclear. We further found that in 50% of these anaphase cells, Pavarotti-KLP was detected at indentations of the cell cortex, suggesting that contraction had occurred (Fig. 7B, panel 2). In telophase-like cells, a diffuse staining was found at the defective central spindle region (Fig. 7B, panel 3). This Pavarotti-KLP signal, although weaker than that seen in control cells was present in some cells undergoing telophase (panel 4) and cytokinesis (panel 5). This signal was concomitant with microtubule bundling. This strongly suggests that in *Glued* RNAi cells, the recruitment of Pavarotti-KLP to the plus ends of microtubules and consequently the microtubule bundle formation were delayed rather than completely inhibited, leading to abnormal but successful cytokinesis.

Analysis of mitosis in live cells

Previous observations of fixed preparations suggested that the early recruitment of Pavarotti-KLP to the plus ends of central spindle microtubules, and the consequent microtubule bundling were delayed during early anaphase. However, it seemed that a minimal but sufficient amount of Pavarotti-KLP was able to promote central spindle formation during telophase, allowing cytokinesis to occur. Thus we decided to monitor mitosis in live cells expressing GFP-tagged α-tubulin following control or *Glued* dsRNA transfection.

In control cells, the time between nuclear envelope breakdown (NEBD) and anaphase onset was 31.1±7.1 minutes (n=16 cells, see also Fig. 8A and supplementary material Movie 1). Consistent with our fixed cell observations, we

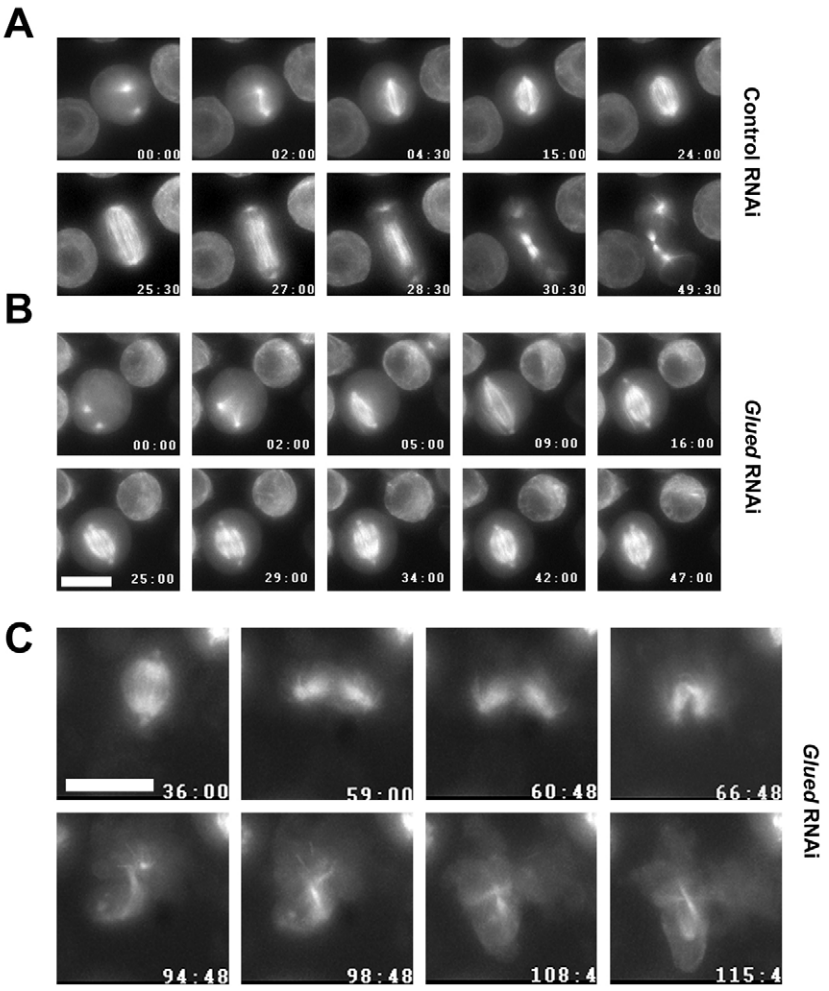

Fig. 8. Following *Glued* RNAi, centrosomes are not properly attached to spindle poles during spindle formation and microtubule bundling is defective after anaphase. Selected frames from time-lapse series of a control cell (A, see also supplementary material Movie 1) or a *Glued* dsRNA treated cell (B,C and supplementary material Movies 2 and 3) expressing GFP-tagged α tubulin during mitosis. (A) Mitosis of a control cell. (B) Mitotic spindle formation following nuclear envelope breakdown until metaphase in a *Glued* dsRNA-treated cell. Note the poor centrosome connection to the spindle poles. (C) Metaphase-to-anaphase transition in a *Glued* dsRNA-treated cell. To avoid long light exposure and radiation damage, the acquisition started at metaphase. Note the lack of microtubule bundles during anaphase (60:48). The cell is also subjected to strong cortex contraction but is able to organise a central spindle region and a midbody (115:4). The panels are maximum projections of *Z* series and note that at time 66:48 the two poles are not in the same focal plane. The time scale (minutes: seconds) is shown at the bottom of each panel. Bars, 10 μm.

frequently found (9 out of 15 cells filmed) centrosome disconnection from the spindle poles before anaphase (Fig. 8B and supplementary material Movie 2) following *Glued* dsRNA treatment. Filming further revealed a metaphase arrest and none of the 15 cells monitored entered anaphase within the 65-minute recording period. We therefore identified cells that were already in metaphase and began filming at that stage. Upon anaphase entry, spindles became distorted and buckled (Fig. 8C and supplementary material Movie 3). At no point did we observe the accumulation of large numbers of microtubules or microtubule bundles as seen in control cells. Cytokinesis could initiate however and, as shown in Fig. 8C, the cortex could constrict and a midbody formed. Thus, depletion of *Glued* leads to post-anaphase spindle deformation and delayed and reduced central spindle microtubule bundle formation.

Discussion

Contribution of DDC to synchronous chromosome segregation

Here we show that in *Drosophila* cultured cells, knockdown of $p150^{Glued}$ leads to a metaphase arrest and after the eventual transition into anaphase, disrupts chromosome segregation and central spindle formation. Previous studies have shown that perturbation of other DDC subunits can disengage the centrosomes from metaphase spindles in both tissue culture cells and mutant neuroblasts (Goshima et al., 2005; Morales-Mulia and Scholey, 2005; Siller et al., 2005). Likewise our study confirms a role for the DDC in timely anaphase entry.

We found that half of the p150 knock down cells shared a common phenotype during karyokinesis. In addition, spindles were long and some chromosomes were clustered at the poles while others remained at the spindle equator. While this phenotype is suggestive of cells with chromosome congression defects, several lines of evidence suggest that these are aberrant anaphases: (1) we consistently found that such abnormal cells had cyclin B levels that were indistinguishable from anaphase controls; (2) the centromeric protein MEI-S322, which is lost from anaphase centromeres, was not detected on those chromosomes which were adjacent to the spindle poles, but was detectable on chromosomes lagging at the equator; (3) the chromosome passenger protein Aurora B, which redistributes to the spindle equator following anaphase onset for successful cytokinesis (see below), was lacking on polar proximal chromosomes but could still be detected on the centromeres of those chromosomes at the cells centre; and (4) when cells were stained for the spindle checkpoint protein BubR1, the signal intensity at kinetochores found near the spindle poles was identical to those observed in control anaphase cells, whereas the fluorescent signal on the kinetochores seen at the spindle equator was similar to that observed during metaphase. Taken

together, these data strongly suggest that the depletion of p150^{Glued} by RNAi distorts anaphase, allowing some chromosomes to undergo their normal maturation (i.e. loss of checkpoint and centromeric proteins followed by disjunction and segregation to the poles), while others are inhibited from initiating this series of events.

Our observations indicate that the disappearance of Aurora B, MEI-S322 and BubR1 from the centromeres/inner kinetochores may be not be fully dependent on the global loss of MPF activity (note that most cyclin B is degraded in *Glued* anaphase cells). This suggests that DDC does not influence the initial accumulation of cyclin B on the spindle or kinetochore regions, and is not involved in the degradation of the spindle-associated pool. However, the retention of Aurora B, MEI-S332 and BubR1 at kinetochores in *Glued*-depleted cells suggests that the DDC is needed for removal of these proteins and for anaphase onset/chromatid disjunction. How the DDC regulates this is unclear. A pool of BubR1 localises to the inner region of the kinetochore (Buffin et al., 2005; Jablonski et al., 1998) where it interacts with Aurora B (Lampson and Kapoor, 2005). In addition, MEI-S322-dependant phosphorylation by aurora B is required for chromatid cohesion (Resnick et al., 2006). Thus, the loss of p150^{glued} and DCC function may prevent these interactions and the loss or redistribution of key proteins for chromatid cohesion and subsequent chromosome segregation. In addition, previous studies have revealed that a primary function of the DDC, loaded to the kinetochore via the ZW10/Rod complex, is to generate at least in part, poleward chromosome movement during anaphase in many organisms (Savoian et al., 2000; Schmidt et al., 2005; Sharp et al., 2000). Thus, depletion of p150^{Glued} may lead to lagging chromosomes by two methods, in the first, the molecules needed for chromatid disjunction fail to be redistributed and second, there is a failure to secure polewards force generating dynein motor molecules.

Contribution of DDC to central spindle formation

Along with the karyokinetic defects described above, we found that the depletion of *Glued* also disrupted central spindle formation. This microtubule-based structure consists of overlapping anti-parallel arrays of bundled microtubules and a variety of associated proteins and is crucial for successful cytokinesis (D'Avino et al., 2005). Indeed in many instances, only weak indications of a central spindle could be found. In contrast to control cells which always contained robust central spindles and stained positive for Aurora B and polo, the early forming central spindle structures in *Glued* RNAi cells lacked detectable levels of these kinases. These molecules are essential for successful cytokinesis (Adams et al., 1998; D'Avino et al., 2005; Echard et al., 2004; Gatti et al., 2000; Giet and Glover, 2001; Somma et al., 2002), leading to the expectation that cleavage should fail in *Glued* RNAi-treated cells. We failed to detect any octaploid cells or elevated numbers of binucleated cells following *Glued* RNAi in our study, even after a double *Glued* RNAi treatment. In addition, several RNAi screens recently performed in *Drosophila* S2 cells, did not identify any DDC encoding genes essential for cytokinesis (Echard et al., 2004; Eggert et al., 2004) although DDC proteins are found in midbody preparations (Skop et al., 2004). It is thus possible that DDC facilitates central spindle stabilisation and contributes to cytokinesis without being absolutely necessary for this process in flies. Indeed, we found that later-staged cells did localise Aurora B and polo to their central spindle structures, indicating that the DDC facilitates the recruitment of these kinases to the central spindle. In agreement with our findings, a recent study revealed that cytokinesis was not abolished but likewise delayed in sea urchin embryos injected with anti-p150^{Glued} antibodies (Strickland et al., 2005).

Our study further revealed that the DDC is needed for the recruitment of Pavarotti-KLP to the spindle midzone. This kinesin is involved in central spindle formation, furrow formation and ingression by forming a complex with RacGAP50c to form the centralspindlin complex, a master regulator of cytokinesis (D'Avino et al., 2005). Pavarotti-KLP, which concentrates at the overlapping plus ends of microtubules at anaphase onset in control cells, failed to concentrate at the midzone in p150^{Glued} knockdown cells. However, like Aurora B and polo kinases, Pavarotti-KLP did ultimately concentrate on the central spindles and midbodies of later-staged cells. We further observed that Pavarotti-KLP concentrated at the cell cortex in RNAi-treated cells. This may explain the abnormal contractions seen in both fixed and living preparations because it has previously been demonstrated that ectopic expression of this motor protein can promote the recruitment of other furrow components for furrow ingression (Minestrini et al., 2003). Thus, the DDC appears to be responsible for an efficient localisation of Aurora B and polo kinases as well as of Pavarotti-KLP to the central spindle for a timely onset of furrowing.

In summary, we report here for the first time that p150^{Glued}, part of the evolutionarily conserved DDC, is needed for the localised redistribution of the centromeric and/or kinetochore proteins MEI-S332, BubR1 and Aurora B for chromatid disjunction and subsequent segregation. We further show for the first time that p150^{Glued} is involved in cytokinesis. Although not required for successful cell cleavage, our data reveal that *Glued* increases the efficiency of Aurora B and polo kinase recruitment to the midzone for central spindle formation and stabilisation. We further demonstrate that the DDC is needed for the efficient recruitment of Pavarotti-KLP, a member of the centralspindlin complex, which is essential for cell cleavage.

Materials and Methods

dsRNA production and constructs

To generate *Glued* dsRNA, a cDNA fragment was amplified by PCR using the oligonucleotides 5′-ATGTAATACGACTCACTATAGGGCGAATGTCCGAGAA-AAACCTGAAAGTG-3′ and 5′-ATGTAATACGACTCACTATAGGGCGACGA-AGCCTGAGCACCCAT-3′ containing a T7 promoter sequence at each end. The 1100 bp PCR product was used as a template to generate RNA using the Megascript kit (Promega). After isolation, the RNAs were boiled for 20 minutes and annealed by slow cooling overnight at room temperature. dsRNA was analysed by agarose gel electrophoresis and aliquoted at –80°C before use in RNAi experiments.

To generate a construct for expressing GFP-tagged p150^{Glued} in *Drosophila* cells, a PCR fragment was amplified using the oligonucleotides 5′-AAGTCGACG-TACATCAGTTATACCCAC-3′ and 5′-TTGGTACCATTTACCTTTAATATATA-ATATAC-3′ and cloned into pKS-Ub-GFP using *Sal*I and *Kpn*I restriction sites to generate pKS-Ub-GFP-p150^{Glued} (Minestrini et al., 2002).

To produce a recombinant protein used to generate an antibody against the p150^{Glued} protein, a ~450 base pair DNA fragment, encoding the 148 N-terminal domain of p150^{Glued} was amplified by PCR using the oligonucleotides 5′-AAG-AATTCCATGTCCGAGAAAAACCTGAAAGTG-3′ and 5′-AAAAGCTTTTGC-GGCGCCAAAGATTT-3′ and cloned into pET23b using the *Eco*RI and *Hin*dIII restriction sites to generate pET23b-p150$^{Glued\text{-}Nter(His)6}$ expression construct.

Production of recombinant proteins and antibody purification

p150$^{Glued\text{-}Nter(His)6}$ protein was expressed in *E.coli* BL21(DE3)pLysS (Novagen) for

4 hours at 25°C. The protein was purified on a Ni-NTA-agarose column (Qiagen) following the manufacturer's instructions. The purified protein was dialysed overnight against PBS (136 mM NaCl, 26 mM KCl, 2 mM Na_2HPO_4, 2 mM KH_2PO_4, pH 7.2) and used to immunise rabbits to generate Rb1477 and Rb1478 antisera.

Rabbit anti-p150^{Glued} antibodies were affinity purified on nitrocellulose membrane. 1 mg p150Glued$^{-Nter(His)6}$ protein was immobilised on a nitrocellulose membrane. The membrane was incubated for 10 minutes at room temperature in 100 mM glycine-HCl pH 3 to remove unbound protein, then 2 hours in PBS containing 5% BSA and 0.5% Tween 20 (PBST-BSA) for blocking. The membrane was incubated overnight in 20 ml PBST-BSA containing 10% antisera Rb1477 AND Rb1478. After extensive washings in PBST-BSA, specific anti-p150^{Glued} IgG were eluted with 2 ml of 100 mM Glycine-HCl pH 3 for 10 minutes, neutralised with 200 μl of 1M Tris solution, concentrated using a centricon 30 (PAL) and stored at –80°C at 1 μg/ml.

RNAi, transfections, drug treatment and stable line generation

Drosophila S2 cells were grown and processed for RNAi as described previously (Clemens et al., 2000). Briefly, 10^6 cells were incubated with 10 μg/ml dsRNA in serum-free medium. Alternatively, 10 μg Transfast transfection reagent were added together with 3 μg dsRNA following the manufacturer's instructions (Promega). After 1 hour, fresh medium was added to the cells. At 4 days post transfection, the cells were fixed and analysed for mitotic defects (Giet and Glover, 2001). 100-200 mitoses were scored and analysed per experiment, and each experiment was repeated at least three times.

To depolymerise microtubules, S2 cells were treated for 1 hour with 10 μg/ml colchicine (Sigma) before analysis.

To prepare stable lines expressing GFP-tagged 150^{Glued} or GFP-tagged α-tubulin, 10 μg plasmid pKS-Ub-GFP-p150^{Glued} or pAc-GFP-tub (Rogers et al., 2002) was co-transfected with 1 μg pIB/V5-His/CAT or pCoHygro in S2 cells. Stable lines were selected and expanded in medium containing 25 μg/ml blasticidin S or 200 μg/ml hygromycin following the manufacturer's instructions (Life Technologies).

Immunofluorescence analysis

S2 cells were fixed in PHEM buffer (60 mM PIPES, 25 mM HEPES, 10 mM EGTA, 4 mM $MgCl_2$) containing 5% formaldehyde and 0.1% Triton X-100 at room temperature for 10 minutes. For Cyclin B immunofluorescence analyses, the cells were fixed in methanol at –20°C for 10 minutes. The fixed cells were briefly washed in PBS, and blocked for 1 hour in PBS containing 0.1% Triton X-100 and 1% BSA (PBSX-BSA). Primary antibodies were incubated overnight at 4°C and secondary antibodies were incubated for 2 hours at room temperature in PBSX-BSA. DNA was stained with Hoechst 33258. Slides were mounted in Vectashield (Vector Laboratories) and observed with a DMRXA2 microscope (Leica). Images were acquired with a CoolSnapsHQ camera (Photometrics) and processed with Metamorph software (Universal Imaging). Alternatively, images were acquired with a Leica DMIRE2 inverted confocal microscope.

FACS analysis

S2 cells were fixed in PBS containing 70% ethanol and stored at –20°C until analysis. For FACS analysis, S2 ethanol-fixed cells were washed twice in PBS and incubated with PBS containing 40 μg/ml RNAse A and 10 μg/ml propidium iodide for 30 minutes. S2 cells were analysed using a Coulter Epics Elite Flow Cytometer (Beckman Coulter).

Live cell imaging

All time-lapse imaging was performed on a Leica DMIRBE inverted microscope controlled by the Metamorph software using an oil 63× objective (NA 1.40). *Z* series (0.3 μm steps) were acquired at 30 or 60 second intervals with a CoolSnapES camera (Roper Scientific) using a bin of 2. Cells were bathed in a chambered coverglass system (Lab-Tek) and maintained at 25°C.

Antibodies and western blotting

The YL1/2 rat anti-tyrosinated tubulin antibody (dilution 1:100) was from Seralab. The GTU-88 mouse anti-γ-tubulin, the anti-dynein intermediate chain and the anti-GFP monoclonal antibodies (dilution 1:1000) were from Sigma, Chemicon and Roche respectively. Antibodies against Pavarotti-KLP (1:1000), BubR1 (1:3000) MEI-S322 (dilution 1:2000), Aurora B (1:1000), Cyclin B (1:5000) and anti-polo monoclonal antibody (dilution 1:40) were kind gifts from the indicated authors (Adams et al., 1998; Giet and Glover, 2001; Heuer et al., 1995; Kerrebrock et al., 1995; Logarinho et al., 2004; Whitfield et al., 1995). The affinity-purified anti-p150^{Glued} antibody was used at 0.2 μg/ml. Peroxidase-, FITC-, Texas Red- and Cy5-conjugated anti-rabbit, anti-sheep, anti-mouse or anti-rat secondary antibodies were from Jackson, and the Alexa Fluor 488-conjugated antibodies from Molecular Probes. For western blotting, ECL reagent was purchased from Pierce.

We would like to acknowledge S. Dutertre for help with microscopy work, L. Rault for some immunostaining analyses and G. Goshima, D. M. Glover, T. C. Kaufman, T. L. Orr-Weaver, C. Sunkel for reagents. Thanks are also due to M. S. Savoian for his very helpful critical readings of this manuscript and to R. Karess and unknown referees for helpful suggestions. Rennes Métropole supported this work.

References

Adams, R. R., Tavares, A. A., Salzberg, A., Bellen, H. J. and Glover, D. M. (1998). pavarotti encodes a kinesin-like protein required to organize the central spindle and contractile ring for cytokinesis. *Genes Dev.* **12**, 1483-1494.

Askham, J. M., Vaughan, K. T., Goodson, H. V. and Morrison, E. E. (2002). Evidence that an interaction between EB1 and p150(Glued) is required for the formation and maintenance of a radial microtubule array anchored at the centrosome. *Mol. Biol. Cell* **13**, 3627-3645.

Buffin, E., Lefebvre, C., Huang, J., Gagou, M. E. and Karess, R. E. (2005). Recruitment of Mad2 to the kinetochore requires the Rod/Zw10 complex. *Curr. Biol.* **15**, 856-861.

Busson, S., Dujardin, D., Moreau, A., Dompierre, J. and De Mey, J. R. (1998). Dynein and dynactin are localized to astral microtubules and at cortical sites in mitotic epithelial cells. *Curr. Biol.* **8**, 541-544.

Carminati, J. L. and Stearns, T. (1997). Microtubules orient the mitotic spindle in yeast through dynein-dependent interactions with the cell cortex. *J. Cell Biol.* **138**, 629-641.

Clemens, J. C., Worby, C. A., Simonson-Leff, N., Muda, M., Maehama, T., Hemmings, B. A. and Dixon, J. E. (2000). Use of double-stranded RNA interference in Drosophila cell lines to dissect signal transduction pathways. *Proc. Natl. Acad. Sci. USA* **97**, 6499-6503.

Collins, C. A. and Vallee, R. B. (1989). Preparation of microtubules from rat liver and testis: cytoplasmic dynein is a major microtubule associated protein. *Cell Motil. Cytoskeleton* **14**, 491-500.

D'Avino, P. P., Savoian, M. S. and Glover, D. M. (2005). Cleavage furrow formation and ingression during animal cytokinesis: a microtubule legacy. *J. Cell Sci.* **118**, 1549-1558.

Echard, A., Hickson, G. R., Foley, E. and O'Farrell, P. H. (2004). Terminal cytokinesis events uncovered after an RNAi screen. *Curr. Biol.* **14**, 1685-1693.

Eggert, U. S., Kiger, A. A., Richter, C., Perlman, Z. E., Perrimon, N., Mitchison, T. J. and Field, C. M. (2004). Parallel chemical genetic and genome-wide RNAi screens identify cytokinesis inhibitors and targets. *PLoS Biol.* **2**, e379.

Gatti, M., Giansanti, M. G. and Bonaccorsi, S. (2000). Relationships between the central spindle and the contractile ring during cytokinesis in animal cells. *Microsc. Res. Tech.* **49**, 202-208.

Giet, R. and Glover, D. M. (2001). Drosophila aurora B kinase is required for histone H3 phosphorylation and condensin recruitment during chromosome condensation and to organize the central spindle during cytokinesis. *J. Cell Biol.* **152**, 669-682.

Gill, S. R., Schroer, T. A., Szilak, I., Steuer, E. R., Sheetz, M. P. and Cleveland, D. W. (1991). Dynactin, a conserved, ubiquitously expressed component of an activator of vesicle motility mediated by cytoplasmic dynein. *J. Cell Biol.* **115**, 1639-1650.

Gonczy, P., Pichler, S., Kirkham, M. and Hyman, A. A. (1999). Cytoplasmic dynein is required for distinct aspects of MTOC positioning, including centrosome separation, in the one cell stage Caenorhabditis elegans embryo. *J. Cell Biol.* **147**, 135-150.

Goshima, G. and Vale, R. D. (2003). The roles of microtubule-based motor proteins in mitosis: comprehensive RNAi analysis in the Drosophila S2 cell line. *J. Cell Biol.* **162**, 1003-1016.

Goshima, G. and Vale, R. D. (2005). Cell cycle-dependent dynamics and regulation of mitotic kinesins in Drosophila S2 cells. *Mol. Biol. Cell* **16**, 3896-3907.

Goshima, G., Nedelec, F. and Vale, R. D. (2005). Mechanisms for focusing mitotic spindle poles by minus end-directed motor proteins. *J. Cell Biol.* **171**, 229-240.

Heuer, J. G., Li, K. and Kaufman, T. C. (1995). The Drosophila homeotic target gene centrosomin (cnn) encodes a novel centrosomal protein with leucine zippers and maps to a genomic region required for midgut morphogenesis. *Development* **121**, 3861-3876.

Jablonski, S. A., Chan, G. K., Cooke, C. A., Earnshaw, W. C. and Yen, T. J. (1998). The hBUB1 and hBUBR1 kinases sequentially assemble onto kinetochores during prophase with hBUBR1 concentrating at the kinetochore plates in mitosis. *Chromosoma* **107**, 386-396.

Karess, R. (2005). Rod-Zw10-Zwilch: a key player in the spindle checkpoint. *Trends Cell Biol.* **15**, 386-392.

Karki, S. and Holzbaur, E. L. (1999). Cytoplasmic dynein and dynactin in cell division and intracellular transport. *Curr. Opin. Cell Biol.* **11**, 45-53.

Kerrebrock, A. W., Moore, D. P., Wu, J. S. and Orr-Weaver, T. L. (1995). Mei-S332, a Drosophila protein required for sister-chromatid cohesion, can localize to meiotic centromere regions. *Cell* **83**, 247-256.

Koonce, M. P., Kohler, J., Neujahr, R., Schwartz, J. M., Tikhonenko, I. and Gerisch, G. (1999). Dynein motor regulation stabilizes interphase microtubule arrays and determines centrosome position. *EMBO J.* **18**, 6786-6792.

Lampson, M. A. and Kapoor, T. M. (2005). The human mitotic checkpoint protein BubR1 regulates chromosome-spindle attachments. *Nat. Cell Biol.* **7**, 93-98.

Logarinho, E., Bousbaa, H., Dias, J. M., Lopes, C., Amorim, I., Antunes-Martins, A. and Sunkel, C. E. (2004). Different spindle checkpoint proteins monitor microtubule attachment and tension at kinetochores in Drosophila cells. *J. Cell Sci.* **117**, 1757-1771.

Mathe, E., Kraft, C., Giet, R., Deak, P., Peters, J. M. and Glover, D. M. (2004). The E2-C vihar is required for the correct spatiotemporal proteolysis of cyclin B and itself undergoes cyclical degradation. *Curr. Biol.* **14**, 1723-1733.

Minestrini, G., Mathe, E. and Glover, D. M. (2002). Domains of the Pavarotti kinesin-

like protein that direct its subcellular distribution: effects of mislocalisation on the tubulin and actin cytoskeleton during Drosophila oogenesis. *J. Cell Sci.* **115**, 725-736.

Minestrini, G., Harley, A. S. and Glover, D. M. (2003). Localization of Pavarotti-KLP in living Drosophila embryos suggests roles in reorganizing the cortical cytoskeleton during the mitotic cycle. *Mol. Biol. Cell* **14**, 4028-4038.

Morales-Mulia, S. and Scholey, J. M. (2005). Spindle pole organization in Drosophila S2 cells by Dynein, abnormal spindle protein (Asp), and KLP10A. *Mol. Biol. Cell* **16**, 3176-3186.

Niccoli, T., Yamashita, A., Nurse, P. and Yamamoto, M. (2004). The p150-Glued Ssm4p regulates microtubular dynamics and nuclear movement in fission yeast. *J. Cell Sci.* **117**, 5543-5556.

Resnick, T. D., Satinover, D. L., Macisaac, F., Stukenberg, P. T., Earnshaw, W. C., Orr-Weaver, T. L. and Carmena, M. (2006). INCENP and Aurora B promote meiotic sister chromatid cohesion through localization of the shugoshin MEI-S332 in Drosophila. *Dev. Cell* **11**, 57-68.

Robinson, J. T., Wojcik, E. J., Sanders, M. A., McGrail, M. and Hays, T. S. (1999). Cytoplasmic dynein is required for the nuclear attachment and migration of centrosomes during mitosis in Drosophila. *J. Cell Biol.* **146**, 597-608.

Salina, D., Bodoor, K., Eckley, D. M., Schroer, T. A., Rattner, J. B. and Burke, B. (2002). Cytoplasmic dynein as a facilitator of nuclear envelope breakdown. *Cell* **108**, 97-107.

Savoian, M. S., Goldberg, M. L. and Rieder, C. L. (2000). The rate of poleward chromosome motion is attenuated in Drosophila zw10 and rod mutants. *Nat. Cell Biol.* **2**, 948-952.

Schmidt, D. J., Rose, D. J., Saxton, W. M. and Strome, S. (2005). Functional analysis of cytoplasmic dynein heavy chain in Caenorhabditis elegans with fast-acting temperature-sensitive mutations. *Mol. Biol. Cell* **16**, 1200-1212.

Sharp, D. J., Rogers, G. C. and Scholey, J. M. (2000). Cytoplasmic dynein is required for poleward chromosome movement during mitosis in Drosophila embryos. *Nat. Cell Biol.* **2**, 922-930.

Siller, K. H., Serr, M., Steward, R., Hays, T. S. and Doe, C. Q. (2005). Live imaging of Drosophila brain neuroblasts reveals a role for Lis1/dynactin in spindle assembly and mitotic checkpoint control. *Mol. Biol. Cell* **16**, 5127-5140.

Skop, A. R., Liu, H., Yates, J., 3rd, Meyer, B. J. and Heald, R. (2004). Dissection of the mammalian midbody proteome reveals conserved cytokinesis mechanisms. *Science* **305**, 61-66.

Somma, M. P., Fasulo, B., Cenci, G., Cundari, E. and Gatti, M. (2002). Molecular dissection of cytokinesis by RNA interference in Drosophila cultured cells. *Mol. Biol. Cell* **13**, 2448-2460.

Strickland, L. I., Wen, Y., Gundersen, G. G. and Burgess, D. R. (2005). Interaction between EB1 and p150(glued) is required for anaphase astral microtubule elongation and stimulation of cytokinesis. *Curr. Biol.* **15**, 2249-2255.

Vallee, R. B. and Stehman, S. A. (2005). How dynein helps the cell find its center: a servomechanical model. *Trends Cell Biol.* **15**, 288-294.

Vallee, R. B., Shpetner, H. S. and Paschal, B. M. (1989). The role of dynein and other microtubule-activated ATPases in mitosis. *Prog. Clin. Biol. Res.* **318**, 205-215.

Vallee, R. B., Vaughan, K. T. and Echeverri, C. J. (1995). Targeting of cytoplasmic dynein to membranous organelles and kinetochores via dynactin. *Cold Spring Harb. Symp. Quant. Biol.* **60**, 803-811.

Vaughan, P. S., Miura, P., Henderson, M., Byrne, B. and Vaughan, K. T. (2002). A role for regulated binding of p150(Glued) to microtubule plus ends in organelle transport. *J. Cell Biol.* **158**, 305-319.

Whitfield, W. G., Chaplin, M. A., Oegema, K., Parry, H. and Glover, D. M. (1995). The 190 kDa centrosome-associated protein of Drosophila melanogaster contains four zinc finger motifs and binds to specific sites on polytene chromosomes. *J. Cell Sci.* **108**, 3377-3387.

Journal of Cell Science